Journal of Solid Mechanics Vol. 3, No. 2 (2011) pp. 198-207

# Effect of Boundary Condition on Pre-Existing Crack Under Fatigue Loading

V.K. Singh*, P.C. Gope, R.K. Bhagat

*Department of Mechanical Engineering, College of Technology, Govind Ballabh Pant University of Agriculture & Technology, Pantnagar- 263 145, India*

Received 12 June 2011; accepted 28 July 2011

**ABSTRACT**

In this paper, the present investigation has been conducted keeping in mind some of the problems concerning the crack propagation direction and growth under constant loading in an inclined crack geometry. The present studies mainly focused on the development and modifications in the crack growth criterion to account the biaxial, shear loading and number of stress terms. Existing criteria for the prediction of crack initiation direction have been modified taking higher order stress terms. The effective methods of experimentally determining the stress intensity factor for a body containing a crack is to analyze the isochromatic pattern obtained from a photoelastic model. The effect of biaxial load factor, crack angle, Crack length/width of specimen and length of specimen/width of specimen were studied and a regression model was developed for geometry correction to predict stress intensity factor for tearing mode and intensity factor for shearing mode. This approach is being used to predict crack growth trajectory under biaxial cyclic loading by assuming that the crack may grow in a number of discrete steps using the vectorial method. MTS criterion (Maximum Tangential Stress criterion) is used for prediction of crack initiating angle. The crack growth trajectory has been determined by cycle simulation procedure.



**Keywords:** Stress intensity factor; Crack growth; Photo elasticity

## 1 INTRODUCTION

THE strength of a structure could be severely affected by presence of crack like defects or pre-existing cracks and the defects are unavoidable in a cost effective manufacturing process. Since there are limitations on minimum size of the defects that can be detected, one needs to know the relation between the defect size and the strength of a structure. Fracture mechanics provide a methodology through which a quantitative relationship between the applied stress on a structure, defects size present, inherent properties of material and the fracture resistance characteristics of structure may be obtained.

In the middle 1950 Irwin and co-workers laid the foundations for what has since become known as fracture mechanics [1]. The most important contribution of this development has been to introduce and experimentally determined material constant called the stress intensity factor ($K$) that characterizes the significance of the defects present in a material from the point of view of brittle crack growth. The effective methods of experimentally determining the stress intensity factor for a body containing a crack is to analyze the isochromatic pattern obtained from a photoelastic model. Measurements of the fringe order $N$ and position parameters $r$ and $\theta$, which locate number of points on a fringe loop, are sufficient to permit the determination of $K_I$ and $K_{II}$. The Irwin method for SIF

* Corresponding author.
*E-mail address:* vks2319@yahoo.co.in (V. K. Singh).

extraction from photoelastic patterns was the accepted method for analysis for many years. In this method, the positional coordinates and fringe order for a specific point that satisfies the criteria is used for evaluating $K_I$ and $K_{II}$.

The crack usually initiates at the surface of the specimen and propagate slowly at first into the interior. This is called as micro crack growth. The material will continue the neck down, the crack is found to nucleate at brittle particle. A particle is said to have nucleated, when it becomes stable and will not disappear due to thermal fluctuation. Once the particle has attained this stage, it can grow further with a continuous decrease in energy. If fracture initiate at pore in the crack region, then the voids are already present. The voids grow with increasing deformation and ultimately reach sizes of the order of millimeter. This is called as macro crack growth. All some critical stage, the crack propagation becomes rapid culminating in fracture. With the recent advances in computation technology, researchers around the globe are working to simulate the crack propagation under different loading conditions.

One can predict the crack propagation path if crack initiation and subsequent crack extension (initiation) angles are known. The problem needs to be studied in mixed mode since in mixed mode loading both crack initiation angle and hence crack growth rate varies during subsequent growth process. Prediction of initial fracture angle of mixed mode problem allows for the determination of the crack trajectory based on strain energy density factor. Several studies related to the prediction of the initial fracture crack angle and crack trajectories under mixed mode loading conditions were performed for uniaxial loadings as well as for biaxial loadings. The strain energy density criterion is to predict the crack trajectory by approximating the developed crack by new crack angle and a fictitious crack length under uniaxial loading. Later, this approach is being used to predict crack growth trajectory under biaxial cyclic loading by assuming that the crack may grow in a number of discrete steps using the vectorial method.

The objective and focus of the current research is to characterize the fatigue crack growth behaviour under different boundary conditions. Evaluation of the equations and photoelastic techniques is used for this study. The development of the equations used in this study will start from basic fracture mechanics, which will then be substituted into to photoelastic equations. An investigation into the effects of both crack length and boundary conditions on photoelastic materials is performed. Specimens containing various crack lengths and boundary conditions are analyzed using common photoelastic techniques. A new technique is developed for data collection for photoelastic analysis.

## 2 ANALYSIS OF THE PROBLEM

The stress optic law relates the fringe order $N$ and principal stresses $\sigma_1$ and $\sigma_2$ as [2]:

$$\frac{Nf_\sigma}{t} = \sigma_1 - \sigma_2 \tag{1}$$

where $f_\sigma$ is the material fringe value and t is the model thickness. For a plane stress problem, the principal stresses are [3]:

$$\sigma_1, \sigma_2 = \frac{\sigma_x + \sigma_y}{2} \pm \sqrt{\frac{(\sigma_x + \sigma_y)^2}{4} + (\sigma_{xy})^2} \tag{2}$$

For the purpose of mixed mode study, the stresses in the local neighborhood of a crack tip ($r/a$<1) can be approximated by *Westergaard* Stress component $\sigma_{ij}$ in an increasing order power series as follows [4]:

$$\sigma_x = \sigma_{ox} + \frac{K_1}{2\sqrt{\pi a}}\left\{\left(\frac{r}{2a}\right)^{-1/2}\cos\frac{\theta}{2}\left(1-\sin\frac{\theta}{2}\sin\frac{3\theta}{2}\right)\right.$$
$$\left. + \frac{3}{2}\left(\frac{r}{2a}\right)^{1/2}\cos\frac{\theta}{2}\left(1+\sin^2\frac{\theta}{2}\right) + \sum_{n=1}^{\infty}\left(\frac{r}{2a}\right)^{n+1/2} C_n\left[\cos\left(n+\frac{1}{2}\right)\theta - \left(n+\frac{1}{2}\right)\sin\theta\sin\left(n-\frac{1}{2}\right)\theta\right]\right\}$$

$$+\frac{K_{11}}{2\sqrt{\pi a}}\left\{-\left(\frac{r}{2a}\right)^{-1/2}\sin\frac{\theta}{2}\left(2+\cos\frac{\theta}{2}\cos\frac{3\theta}{2}\right)\right.$$
$$\left.+\frac{3}{2}\left(\frac{r}{2a}\right)^{1/2}\sin\frac{\theta}{2}\left(2+\cos^2\frac{\theta}{2}\right)+\sum_{n=1}^{\infty}\left(\frac{r}{2a}\right)^{n+1/2}C_n\left[2\sin\left(n+\frac{1}{2}\right)\theta+\left(n+\frac{1}{2}\right)\sin\theta\cos\left(n-\frac{1}{2}\right)\theta\right]\right\} \quad (3)$$

$$\sigma_y=\frac{K_1}{2\sqrt{\pi a}}\left\{\left(\frac{r}{2a}\right)^{-1/2}\cos\frac{\theta}{2}\left(1+\sin\frac{\theta}{2}\sin\frac{3\theta}{2}\right)+\frac{3}{2}\left(\frac{r}{2a}\right)^{1/2}\cos^3\frac{\theta}{2}\right.$$
$$\left.+\sum_{n=1}^{\infty}\left(\frac{r}{2a}\right)^{n+1/2}C_n\left[\cos\left(n+\frac{1}{2}\right)\theta+\left(n+\frac{1}{2}\right)\sin\theta\sin\left(n-\frac{1}{2}\right)\theta\right]\right\}$$
$$+\frac{K_{11}}{2\sqrt{\pi a}}\left\{\left(\frac{r}{2a}\right)^{-1/2}\sin\frac{\theta}{2}\cos\frac{\theta}{2}\cos\frac{3\theta}{2}-\frac{3}{2}\left(\frac{r}{2a}\right)^{1/2}\sin\frac{\theta}{2}\cos^2\frac{\theta}{2}\right.$$
$$\left.-\sum_{n=1}^{\infty}\left(\frac{r}{2a}\right)^{n+1/2}C_n\left(n+\frac{1}{2}\right)\sin\theta\cos\left(n-\frac{1}{2}\right)\theta\right\} \quad (4)$$

$$\sigma_{xy}=\frac{K_1}{2\sqrt{\pi a}}\left\{\left(\frac{r}{2a}\right)^{-1/2}\sin\frac{\theta}{2}\cos\frac{\theta}{2}\cos\frac{3\theta}{2}-\frac{3}{2}\left(\frac{r}{2a}\right)^{1/2}\sin\frac{\theta}{2}\cos^2\frac{\theta}{2}\right.$$
$$\left.-\sum_{n=1}^{\infty}\left(\frac{r}{2a}\right)^{n+1/2}C_n\left(n+\frac{1}{2}\right)\sin\theta\cos\left(n-\frac{1}{2}\right)\theta\right\}+\frac{K_{11}}{2\sqrt{\pi a}}\left\{\left(\frac{r}{2a}\right)^{-1/2}\right.$$
$$\cos\frac{\theta}{2}\left(1-\sin\frac{\theta}{2}\sin\frac{3\theta}{2}\right)+\frac{3}{2}\left(\frac{r}{2a}\right)^{1/2}\cos\frac{\theta}{2}\left(1+\sin^2\frac{\theta}{2}\right)$$
$$\left.+\sum_{n=1}^{\infty}\left(\frac{r}{2a}\right)^{n+\frac{1}{2}}C_n\left[\cos\left(n+\frac{1}{2}\right)\theta-\left(n+\frac{1}{2}\right)\sin\theta\sin\left(n-\frac{1}{2}\right)\theta\right]\right\} \quad (5)$$

where $\sigma_{ox}$ and $a$ are constant stress field and half crack length, respectively, $r$ and $\theta$ are polar co-ordinates with the origin defined at the crack tip and $C_n=(-1)^n\left(\frac{2n+3}{2n+2}\right)\frac{1\times3\times.....\times(2n-1)}{2\times4\times.....2n}$.

The maximum in-plane shear stress ($\tau_m$) is related to the Cartesian components of stress by [3]:

$$(2\tau_m)^2=(\sigma_y-\sigma_x)^2+(2\sigma_{xy})^2 \quad (6)$$

Eq. (6) re-writing as

$$(\sigma_1-\sigma_2)^2=(\sigma_y-\sigma_x)^2+(2\sigma_{xy})^2 \quad (7)$$

Substituting Eq. (1) in above equation

$$\left(\frac{Nf_\sigma}{t}\right)^2=(\sigma_y-\sigma_x)^2+(2\sigma_{xy})^2 \quad (8)$$

Substituting Eqs. (3)-(5) into Eq. (8), we get

$$\left(\frac{N.f\sigma}{t}\right)^2 = \left\{\frac{K_I}{2\sqrt{\pi a}}\left\{\left(\frac{r}{2a}\right)^{-1/2}\cos\frac{\theta}{2}\left(2\sin\frac{\theta}{2}\sin\frac{3\theta}{2}\right)+3\left(\frac{r}{2a}\right)^{1/2}\cos^3\frac{\theta}{2}-\right.\right.$$
$$3\left(\frac{r}{2a}\right)^{1/2}\cos\frac{\theta}{2}+\sum_{n=1}^{\infty}\left(\frac{r}{2a}\right)^{n+\frac{1}{2}}C_n\left[2\left(n+\frac{1}{2}\right)\sin\theta\sin\left(n-\frac{1}{2}\right)\theta\right]\Bigg\}$$
$$+\frac{K_{II}}{2\sqrt{\pi a}}\left\{\left(\frac{r}{2a}\right)^{-1/2}\left(2\sin\frac{\theta}{2}\cos\frac{\theta}{2}\cos\frac{3\theta}{2}\right)+\left(\frac{r}{2a}\right)^{-1/2}2\sin\frac{\theta}{2}-\frac{3}{2}\right.$$
$$\left(\frac{r}{2a}\right)^{\frac{1}{2}}2\sin\frac{\theta}{2}\cos^2\frac{\theta}{2}-\frac{3}{2}\left(\frac{r}{2a}\right)^{1/2}2\sin\frac{\theta}{2}$$
$$\left.\left.-\sum_{n=1}^{\infty}\left(\frac{r}{2a}\right)^{n+\frac{1}{2}}C_n\left[2\sin\left(n-\frac{1}{2}\right)\theta\right]-\sigma_{0x}\right\}\right\}^2$$
$$+\left\{\frac{K_1}{2\sqrt{\pi a}}\left\{\left(\frac{r}{2a}\right)^{-1/2}\sin\frac{\theta}{2}\cos\frac{\theta}{2}\cos\frac{3\theta}{2}-\frac{3}{2}\left(\frac{r}{2a}\right)^{1/2}\sin\frac{\theta}{2}\cos^2\frac{\theta}{2}\right.\right.$$
$$\left.-\sum_{n=1}^{\infty}\left(\frac{r}{2a}\right)^{n+1/2}C_n\left(n+\frac{1}{2}\right)\sin\theta\cos\left(n-\frac{1}{2}\right)\theta\right\}+\frac{K_{11}}{2\sqrt{\pi a}}\left\{\left(\frac{r}{2a}\right)^{-1/2}\right.$$
$$\cos\frac{\theta}{2}\left(1-\sin\frac{\theta}{2}\sin\frac{3\theta}{2}\right)+\frac{3}{2}\left(\frac{r}{2a}\right)^{1/2}\cos\frac{\theta}{2}\left(1+\sin^2\frac{\theta}{2}\right)$$
$$\left.\left.+\sum_{n=1}^{\infty}\left(\frac{r}{2a}\right)^{n+\frac{1}{2}}C_n\left[\cos\left(n+\frac{1}{2}\right)\theta-\left(n+\frac{1}{2}\right)\sin\theta\sin\left(n-\frac{1}{2}\right)\theta\right]\right\}\right\}^2 \tag{9}$$

The N-K relation given in Eq. (9) is non-linear in term of the three unknowns $K_I$, $K_{II}$ and $\sigma_{ox}$. In the present analysis, three points deterministic approach have been used. The Newton-Raphson-method [5] is applied to solve three simultaneous non-linear equations. All the experimental work has been done on photo elastic material, casted by using Resin (CY-230) and Hardener (HY-951).

In this approach, data is selected from three arbitrary points ($r_1$, $\theta_1$), ($r_2$, $\theta_2$) and ($r_3$, $\theta_3$) on a fringe loop by the help of new developed image processing technique. To minimize the error for data collection, a new method of image processing for accurate measurement of the ($r$, $\theta$) are presented in Fig. 1.

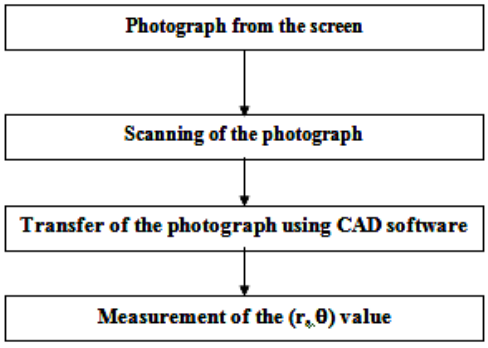


**Fig. 1**
Flow chart of image processing procedure.

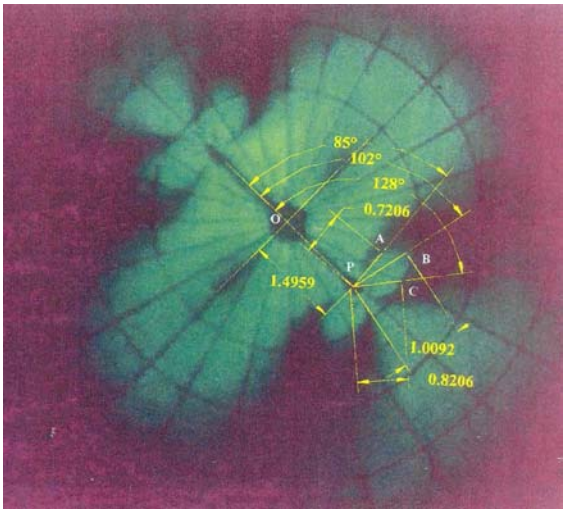


**Fig. 2**
Image processing and measurement of fringe position from crack tip using CAD software.

For this purpose, photograph from the screen of the photoelastic bench under different loading condition were taken and scanned by the help of scanner. The scanned photographs were loaded in CAD software for the measurement of ($r$, $\theta$) at the different points from the crack-tip. Fig. 2 shows three points on the fringe pattern A, B and C, respectively. OP distance shows the half crack length '$a$'. OP is the known distance, used for making a conversion formula of distance measurement in the scanned photographs.

## 3 THE DETERMINATION OF DIRECTION OF CRACK INITIATION

MTS-criterion is the simplest of all, and it states that direction of crack initiation coincides with the direction of the maximum tangential stress along its constant radius around the crack tip. It can be stated mathematically as [6]:

$$(\partial\sigma_\theta / \partial\theta)_{\theta=\theta_0} = 0 \tag{10}$$

$$(\partial^2\sigma_\theta / \partial\theta^2) < 0 \tag{11}$$

Using the stress field in polar co-ordinates and applying the M.T.S.-criterion, we get the following Eq. (6):

$$\tan^2(\theta/2) - (\mu/2)\tan(\theta/2) - 0.5 = 0 \tag{12}$$

$$(-3/2)[\{(1/2)\cos^3(\theta/2)\cos(\theta/2)\sin^2(\theta/2)\} + \{(1/\mu)\sin^3(\theta/2) - (7/2)\sin(\theta/2)\cos^3(\theta/2)\}] < 0 \tag{13}$$

where $\mu$ is defined as,

$$\mu = (K_I / K_{II}) \tag{14}$$

If the value of $\theta$ is equal to the $\beta$, the solution of above equation will give the value of crack initiation angle $\beta_0$.

To solve the equations for the crack initiation angles defined above, we need to have expressions for the stress intensity factors for the angled crack problem for different loading conditions. $\sigma_n$ and $\tau_n$ are the normal and tangential stress to the crack plane respectively. To obtain expressions for $\sigma_n$ and $\tau_n$ for slant crack problem, the most general loading case is considered in Fig. 4.

$$\sigma_n = \sigma_x \cos^2 \beta + \sigma_y \sin^2 \beta - \tau_{xy} \sin 2\beta \tag{15}$$

$$\tau_n = ((\sigma_x - \sigma_y)/2) \sin 2\beta - \tau_{xy} \cos 2\beta \tag{16}$$

The crack growth rate d*a*/d*N* can be expressed as a function of strain energy density range similar to *Paris's law* [7] of mode I cyclic loading and is given by

$$\begin{aligned} (\mathrm{d}a/\mathrm{d}N) &= C(\Delta S)^n \\ &= 2.98x10^{-10}(\Delta S)^{1.15} \quad \text{for} \quad 750 < \Delta S < \Delta S_{cr} \\ &= 1.88x10^{-18}(\Delta S)^{3.98} \quad \text{for} \quad \Delta S < 750 \end{aligned} \tag{17}$$

where $C$ and $\boldsymbol{n}$ are material properties to be determined experimentally, The strain energy density factor range, $\Delta S$, can be expressed as:

$$\Delta S = b_{11}K_I^2 + 2b_{12}K_I K_{II} + b_{22}K_{II}^2 \tag{18}$$

where coefficients $b_{11}$, $b_{12}$ and $b_{22}$ are given by

$$b_{11} = (1/16G)[(1+\cos\beta)(K-\cos\beta)] \tag{19}$$

$$b_{12} = (1/16G)\ \sin\beta[2\cos\beta - (K-1)] \tag{20}$$

$$b_{22} = (1/16G)[(K+1)(1-\cos\beta) + (1+\cos\beta)(3\cos\beta - 1)] \tag{21}$$

where $G$ is modulus of rigidity (N/m$^2$) and k is unit less constant. '$K$ is written in terms of Poisson ratio, given as

$$K = (3-5\upsilon) \quad \text{for plane strain [3]} \tag{22}$$

$$K = (3-\upsilon)/(1+\upsilon) \quad \text{for plane stress [3]} \tag{23}$$

Strain Energy Density range was found to be a convenient parameter for predicting fatigue crack growth under complex loading. Using crack geometry, the crack angle and the corresponding crack length at *i*th state of cycle can be expressed in terms of initial fracture crack angle and the incremental crack length given in Fig. 4 as follows:

New crack inclination angle (after crack propagation)

$$\beta_i = \beta + \tan^{-1}[(\Delta a\ \sin\beta_0)(a + \Delta a\ \cos\beta_0)] \tag{24}$$

New half crack length (after crack propagation)

$$a_i = \sqrt{[(\Delta a\ \sin\beta_0)^2 + (a + \Delta a\ \cos\beta_0)^2]} \tag{25}$$

## 4 RESULTS AND DISCUSSIONS

### *4.1 Stress intensity factor, $K_I$*

The effect of biaxial load factor k, crack angle *a*/*W* ratio on stress intensity factor ($K_I$) is shown in Figs. 5-7 for different crack length and crack angles. Figs. 5-7 show that $K_I$ increases as k increases. This may be due to increase in plastic zone size produced ahead of the crack-tip. Figs. 8-10 show that $K_I$ decreases as crack angle $\alpha$ increases for all values of *k*. This may be due to the change of crack position for minimum loading direction ($\sigma$-axis) to maximum loading direction ($k\sigma$-axis). $K_I$ increases when *a*/*W* increases shown in Fig. 7.

The theoretical relation available for $K_I$ is written as [8]:

$$K_I = \frac{\sigma\sqrt{\pi a}}{2}\{(1+k) - (1-k)\cos 2\alpha\} \tag{26}$$

where $k$ denotes stress ratio of maximum load to the minimum load. This relation is based on assumption of infinite plate with remote loading conditions, i.e. $L_e/W_e$=1 for all α values. So that $K_I$ is independent of ($L_e/W_e$) ratio in the above relation. Liebowitz [9] have proposed analytically and numerically that stress intensity factor, depends on the ($L/a$) and ($W/a$), where L is the length of specimen and $W$ is the width of the specimen. In the present investigation, it is seen that $K_I$ depends upon crack angle, biaxial load factor, constant stress term and geometry factor ($a/W$) and ($a/L$). Hence, an attempt has been made to correlate these parameter to $K_I$ and fallowing from is presented.

$$K_I = \sigma\sqrt{\pi a}\left\{(1+k)-(1-k)\cos 2\alpha\right\} f_1\left(\frac{L_e}{W_e}\right) \tag{27}$$

where $L_e$=$L$/2-$a$ cos$\alpha$ and $W_e$=$W$/2-$a$ sin$\alpha$, and the function $f_1$ ($L_e/W_e$) is obtained from regression analysis and found as:

$$f_1\left(\frac{L_e}{W_e}\right)=\left[a_1+a_2\left(\frac{L_e}{W_e}\right)+a_3\left(\frac{L_e}{W_e}\right)^2+a_4\left(\frac{L_e}{W_e}\right)^3+a_5\left(\frac{L_e}{W_e}\right)^4\right] \tag{28}$$

The coefficient ($a_1$ to $a_5$) are shown in Table 1 for various biaxial factor. $L_e$ and $W_e$ are defined in Fig. 3. The correlation coefficient in all cases are found to be greater than 0.90.

*4.2 Stress intensity factor, $K_{II}$*

It reveals from the Fig. 8-10 that $K_{II}$ depends on α, k and (W and L). The magnitude obtained form experiments are also quite different from the theoretical solutions for same boundary conditions and loading. This is due to the geometry constraint. Hence, a geometry factor is derived for $K_{II}$ and presented in the following form [8]:

$$K_{II} = \frac{\sigma\sqrt{\pi a}}{2} f_2\left(\frac{L_e}{W_e}\right) \tag{29}$$

where the function $f_2$ ($L_e/W_e$) is obtained from regression analysis and found as:

**Table 1**
The coefficient of Eq. (28) obtained by regression analysis from the experimental data

| $k$ | Coefficients | | | | |
|---|---|---|---|---|---|
| | $a_1$ | $a_2$ | $a_3$ | $a_4$ | $a_5$ |
| 1.0 | 2958.13 | -12319.36 | 19224.87 | -13324.242 | 3460.51 |
| 1.2 | 4537.08 | 18372.43 | 27972.43 | -18972.07 | 4837.87 |
| 1.4 | 15558.09 | -64654.20 | 100712.02 | -69686.75 | 18072.87 |
| 1.6 | 25511.84 | -105574.57 | 163730.04 | -112775.23 | 29110.39 |
| 1.8 | 13629.04 | -56212.08 | 87054.91 | -59991.82 | 15522.33 |
| 2.0 | 42527.06 | -175971.91 | 272858.97 | -187899.41 | 48486.72 |

**Table 2**
Coefficient of Eq. (30) obtained by regression analysis from the experimental data

| $k$ | Coefficients | | | | |
|---|---|---|---|---|---|
| | $a_{21}$ | $a_{22}$ | $a_{23}$ | $a_{24}$ | $a_{25}$ |
| 1.0 | 0.023338 | -0.006552 | 0.0149691 | -0.103077 | 0.026600 |
| 1.2 | 166886.09 | -484369.54 | 751914.84 | -518243.74 | 133810.83 |
| 1.4 | 52169.22 | -215980.16 | 334828.70 | -230670.93 | 59558.42 |
| 1.6 | 5040.72 | -22239.70 | 36592.78 | -26637.27 | 7234.41 |
| 1.8 | 8273.014 | -34264.72 | 53203.89 | -36704.137 | 9492.012 |
| 2.0 | 2974206.00 | -12400926.00 | 19376463.00 | -13446820.00 | 3497075.30 |

$$f_2\left(\frac{L_e}{W_e}\right)=\left[a_{21}+a_{22}\left(\frac{L_e}{W_e}\right)+a_{23}\left(\frac{L_e}{W_e}\right)^2+a_{24}\left(\frac{L_e}{W_e}\right)^3+a_{25}\left(\frac{L_e}{W_e}\right)^4\right] \tag{30}$$

The coefficients $a_{21}$ to $a_{25}$ are shown in Table 2 for various biaxial factor.

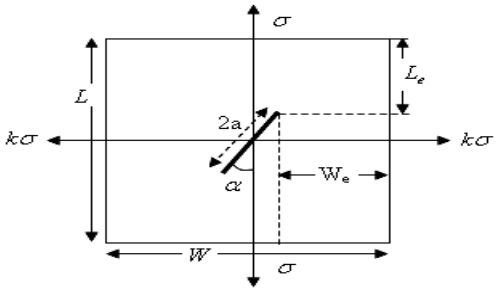


**Fig. 3**
Effective length and effective width in the specimen.

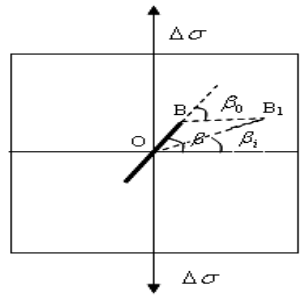


**Fig. 4**
Direction and crack growth.

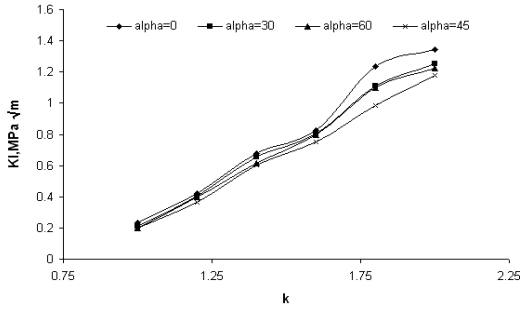


**Fig. 5**
Effect of biaxial factor on stress intensity factor $K_I$ for $a/W$=0.08.

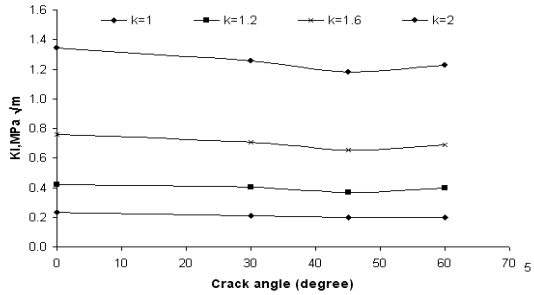


**Fig. 6**
Effect of crack angle on stress intensity factor $K_I$ for $a/W$=0.06.

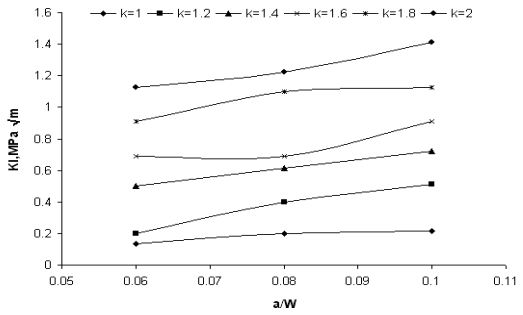


**Fig. 7**
Effect of ($a/W$) ratio on stress intensity factor $K_I$, for $\alpha$=60°.

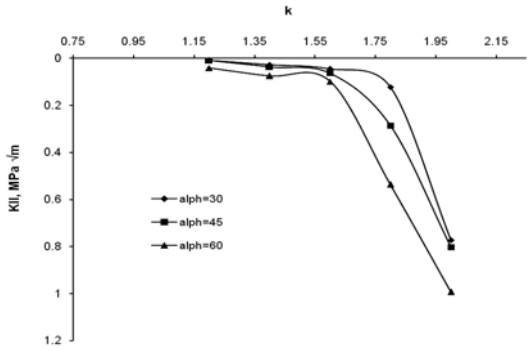


**Fig. 8**
Effect of biaxial factor on stress intensity factor $K_{II}$ for $a/W$=0.08.

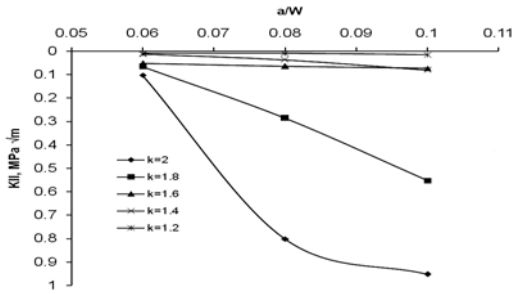


**Fig. 9**
Effect of $a/W$ on stress intensity factor $K_{II}$ for $\alpha = 45^0$.

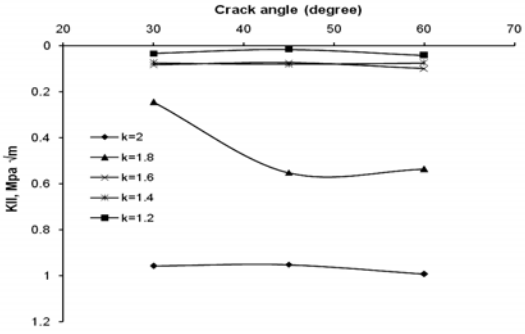


**Fig. 10**
Effect of crack angle on stress intensity factor $K_{II}$ for $a/W$=0.08.

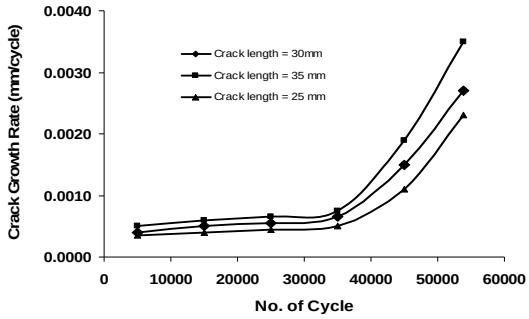


**Fig. 11**
Variation of crack growth rate with number of cycles under different crack length at inclination angle $30^0$.

A detailed analysis has been done under fatigue loading. Maximum Tangential Stress (MTS) criterion has been used for the prediction of crack initiating angle. The crack growth trajectories have been determined by cycle simulation procedure. For determination of instantaneous crack angle and instantaneous crack length, Eq. (24) and Eq. (25) has been used. A computer programme in C++ has been developed to solve the various equations to find out the life and to study the effect of various parameters on fatigue life. The results obtained from the simulation are presented in Fig. 11. Fig. 11 shows a graph between crack growth rate and number of cycles for a constant inclination angle ($30^0$) at different initial crack length. Figure shows that for crack length, initially crack grows slowly and beyond a cycle of $5x10^4$ it increases rapidly. It is observed that as the crack length increases the growth rate also increases beyond the cycle of $5\times10^4$. It is concluded that the life of component depends upon the initial crack length and crack inclination angle and stress intensity factors. According to the Eq. (17) and Eq. (18) crack growth rate increases as the stress intensity factors increases. Stress intensity factors are depended upon the initial crack length, crack angle, biaxial factor k and *a*/*W* as shown in Figs. 5-7 and Figs. 8-10. It is concluded that the life of component depends upon the initial crack length, crack inclination angle biaxial factor k and *a*/*W*. As the crack inclination angle increases the crack growth rate increases and the life of component becomes less. Similarly, as the crack length increases the crack growth rate increases and the life of components decreases. On increasing the value of crack inclination angle the value of new crack length increases for a constant initial crack length.

## REFERENCES

[1] Irwin G.R., 1957, Analysis of stress strains near the end of a crack traversing plate, *ASME Journal of Applied Mechanics* **24**(3): 361-364.
[2] Singh S., 1983, *Applied Stress Analysis*, Khanna Publishers, Second edition, Delhi, India: 346-347.
[3] Nash W., 2007, *Strength of Materials*, McGraw-Hill, Fourth edition, 7.1-7.44, New York.
[4] Ramesh K., Gupta S., Kelkar A.A., 1997, Evaluation of stress field parameter in fracture mechanics by photoelasticity, *Engineering Fracture Mechanics* **56**(1): 25-45.
[5] Kelley L.G., 1991, *Handbook of Numerical Method and Applications*, Addison-Werly, p. 99.
[6] Erdogan F., Sih G.C., 1963, On crack extension in plates under plane loading transverse shear, *ASME Journal of basic Engineering D* **85**: 519-527.
[7] Paris P.C., Erdogan F., 1963, A critical analysis of crack propagation laws, *ASME Journal of basic Engineering D* **85**: 528-533.
[8] Khan Shafique M.A., Khraisheh M.K., 2000, *Analysis of Mixed Mode Crack Initiation Angle under Various Loading Conditions*, Elsevier science Ltd.: 1-10.
[9] Liebowitz H.., Lee J.D., Eftis J., 1978, Biaxial load effects in fracture mechanics, *Engineering Fracture Mechanics* **10**: 315-335.
[10] Stephens R.I., Fatemi A., Stephens R. R., Fuchs H.O., 2001, *Fatigue in Engineering*, Second edition, John Wiley & Sons, Inc., New York.